OPEN

Oncogene (2017) **36**, 6605–6616

www.nature.com/onc

ORIGINAL ARTICLE

The PDGFRα-laminin B1-keratin 19 cascade drives tumor progression at the invasive front of human hepatocellular carcinoma

O Govaere[1,2,7], M Petz[3,7], J Wouters[1], Y-P Vandewynckel[4], EJ Scott[2], B Topal[5], F Nevens[6], C Verslype[6], QM Anstee[2], H Van Vlierberghe[4], W Mikulits[3,7] and T Roskams[1,7]

Human hepatocellular carcinomas (HCCs) expressing the biliary/hepatic progenitor cell marker keratin 19 (K19) have been linked with a poor prognosis and exhibit an increase in platelet-derived growth factor receptor α (PDGFRα) and laminin beta 1 (LAMB1) expression. PDGFRα has been reported to induce *de novo* synthesis of LAMB1 protein in a Sjogren syndrome antigen B (La/SSB)-dependent manner in a murine metastasis model. However, the role of this cascade in human HCC remains unclear. This study focused on the functional role of the PDGFRα-La/SSB-LAMB1 pathway and its molecular link to K19 expression in human HCC. In surgical HCC specimens from a cohort of 136 patients, PDGFRα expression correlated with K19 expression, microvascular invasion and metastatic spread. In addition, PDGFRα expression in pre-operative needle biopsy specimens predicted poor overall survival during a 5-year follow-up period. Consecutive histological staining demonstrated that the signaling components of the PDGFRα-La/SSB-LAMB1 pathway were strongly expressed at the invasive front. K19-positive HCC cells displayed high levels of α2β1 integrin (ITG) receptor, both *in vitro* and *in vivo*. *In vitro* activation of PDGFRα signaling triggered the translocation of nuclear La/SSB into the cytoplasm, enhanced the protein synthesis of LAMB1 by activating its internal ribosome entry site, which in turn led to increased secretion of laminin-111. This effect was abrogated by the PDGFRα-specific inhibitor crenolanib. Importantly LAMB1 stimulated ITG-dependent focal adhesion kinase/Src proto-oncogene non-receptor tyrosine kinase signaling. It also promoted the ITG-specific downstream target Rho-associated coiled-coil containing protein kinase 2, induced K19 expression in an autocrine manner, invadopodia formation and cell invasion. Finally, we showed that the knockdown of LAMB1 or K19 in subcutaneous xenograft mouse models resulted in significant loss of cells invading the surrounding stromal tissue and reduced HepG2 colonization into lung and liver after tail vein injection. The PDGFRα-LAMB1 pathway supports tumor progression at the invasive front of human HCC through K19 expression.

Oncogene (2017) **36,** 6605–6616; doi:10.1038/onc.2017.260; published online 7 August 2017

INTRODUCTION

Liver cancer is the fifth most diagnosed cancer worldwide with an increasing incidence each year, making it the second leading cause of cancer-related death globally.[1] Hepatocellular carcinoma (HCC) represents the major histologic type of primary liver cancer, accounting for 70–85% of the total liver cancer. About 80% of HCCs arise in a background of long-lasting chronic liver disease, making this a heterogeneous disease depending on the underlying etiology and stage of the chronic disease.[2] The Barcelona Clinic Liver Cancer classification system is widely used to stage patients and to guide therapeutic decisions.[3] Only a minority of the patients are eligible for surgical resection or transplantation, largely because of the fact that the majority of HCCs are diagnosed at an advanced stage with macrovascular invasion or metastases.[4] This translates to a 5-year survival of $< 15\%$ for patients diagnosed with HCC. To date, Sorafenib is the only approved drug for systemic treatment of advanced HCC but confers only a modest survival benefit.[5]

In recent years, tremendous efforts have been made to stratify human HCCs based on molecular profiles.[6–8] Although molecular classification of HCC turned out to be useful to predict the outcome of the patient, it has not yet proven helpful in guiding therapeutic choices and management over time.[3] Hoshida and colleagues[9] showed that the gene expression signature in adjacent tissue to HCC correlates with survival, rather than the gene signature from the tumors themselves. This suggests that tumor-surrounding interaction is a pivotal factor in patient-specific prognosis and the progression of HCC. Animal models have shown that the platelet-derived growth factor (PDGF) axis is important in maintaining the invasive phenotype of HCC at the tumor edge.[10] Accordingly, the PDGF receptor alpha (PDGFRα) has been reported to be elevated in human HCC samples, especially in

[1]Department of Imaging and Pathology, KU Leuven and University Hospitals Leuven, Leuven, Belgium; [2]Liver Research Group, Institute of Cellular Medicine, The Medical School, Newcastle University, Newcastle-upon-Tyne, UK; [3]Department of Medicine I, Institute of Cancer Research, Comprehensive Cancer Center, Medical University of Vienna, Vienna, Austria; [4]Department of Hepatology and Gastroenterology, Ghent University, Ghent, Belgium; [5]Department of Abdominal Surgery, KU Leuven and University Hospitals Leuven, Leuven, Belgium and [6]Department of Hepatology, KU Leuven and University Hospitals Leuven, Leuven, Belgium. Correspondence: Dr O Govaere, Liver Research Group, Institute of Cellular Medicine, The Medical School, Framlington Place, Newcastle-upon-Tyne NE2 4HH, UK or Professor W Mikulits, Department of Medicine I, Institute of Cancer Research, Comprehensive Cancer Center, Medical University of Vienna, Borschke-Gasse 8A, Vienna 1090, Austria.
E-mail: olivier.govaere@ncl.ac.uk or wolfgang.mikulits@meduniwien.ac.at
[7]These authors contributed equally to this work.
Received 25 January 2017; revised 30 May 2017; accepted 8 June 2017; published online 7 August 2017

Table 1. Clinical and pathological features of HCC patients ($n = 136$) with correlation to PDGFRA expression

	PDGFRA positive	*PDGFRA negative*
Immunopositivity	66.18% (90/136)	33.82% (46/136)
Age (years) (mean)	63.09 (NS)	60.74 (NS)
Gender		
Male	68.89% (62/90; NS)	71.74% (33/46; NS)
Female	31.11% (28/90; NS)	28.26% (13/46; NS)
Etiology		
HBV	5.56% (5/90; NS)	10.87% (5/46; NS)
HCV	24.44% (22/90; NS)	32.61% (15/46; NS)
HBV+HCV	1.11% (1/90; NS)	6.52% (3/46; NS)
ALD	13.33% (12/90; NS)	17.39% (8/46; NS)
ALD+viral infection	2.22% (2/90; NS)	0% (0/46; NS)
Other	36.66% (33/90; NS)	19.57% (9/46; NS)
Unknown	16.67% (15/90; NS)	13.04% (6/46; NS)
Microvascular invasion	78.89% (71/90; $\mathbf{P < 0.001}$)	19.57% (9/46; NS)
Metastasis	68.18% (45/66; $\mathbf{P < 0.001}$)	20.59% (7/34; NS)
Tumor size (cm; mean)	5.75 ($\mathbf{P < 0.05}$)	3.83
K19 expression	14.44% (13/90; $\mathbf{P < 0.001}$)	0% (0/46; NS)
early HCCs	3.33% (3/90; NS)	26.09% (12/46; NS)
Differentiation grade		
Well	28.89% (26/90)	6.52% (3/46)
Moderate	44.44% (40/90)	32.61% (15/46)
Poorly	26.67% (24/90)	60.87% (28/46)
Cirrhosis		
No	33.33% (30/90; NS)	15.22% (7/46; NS)
Yes	65.56% (59/90; NS)	82.61% (38/46; NS)
Unknown	1.11% (1/90; NS)	2.17% (1/46; NS)

Abbreviations: ALD, alcoholic liver disease; HBV, hepatitis B virus; HCC, hepatocellular carcinoma; HCV, hepatitis C virus; NS, not significant; PDGFRA, platelet-derived growth factor receptor α. Bold values indicate significance.

patient samples diagnosed with microvascular invasion.[11,12] Notably, our recent studies revealed that PDGFRα signaling upregulates the expression of the extracellular matrix protein laminin beta 1 (LAMB1) in a murine model of HCC invasion.[13] LAMB1 is a specific β-chain isoform, which can form, together with an α and γ chain, a trimeric laminin protein that is mainly distributed along the basement membrane. Investigating the regulation of LAMB1 translation, we found that the leader region of the LAMB1 mRNA contains a structural RNA motif that acts as an internal ribosome entry site (IRES) and is regulated by the IRES-transacting factor Sjogren syndrome antigen B (La/SSB).[14] PDGFRα induces the translocation of nuclear La/SSB to the cytoplasm, leading to IRES activation and the increase of LAMB1 *de novo* protein synthesis.[13] We found that this PDGF-La/SSB-LAMB1 axis is induced and maintained by transforming growth factor-β during murine metastasis. In human HCC, we reported that PDGFRα and LAMB1 are associated with keratin (K) 19 expression.[15] The expression of the biliary/hepatic progenitor cell (HPC) marker keratin 19 (K19) is linked with poor prognostic clinicopathological features, such as microvascular invasion, metastasis and early recurrence.[15,16]

This study focuses on the functional role of the PDGFRα-LAMB1 pathway and its molecular link to K19 expression in human HCC progression. We show that PDGFRα expression is increased at the invasive front of human HCC. *In vitro* activation of PDGFRα leads to translational activation of LAMB1, which in turn induces an invasive and metastatic phenotype of tumor cells exhibiting K19 expression. Our findings provide evidence that K19 expression is inducible in human HCC as a sign of tumor progression.

RESULTS

Components of the PDGFRα-La/SSB-LAMB1 signaling pathway are co-expressed at the invasive front of human HCC

In order to evaluate the clinicopathological and prognostic significance of PDGFRα expression, two retrospective, consecutive cohorts were included in this study: one consisting out of surgical specimens ($n = 136$) and one out of needle biopsies ($n = 46$). In the cohort of 136 HCC patients, PDGFRα protein expression was observed at the cellular membrane in 66.2% of the samples (90/136) and correlated significantly with microvascular invasion ($P < 0.001$), metastasis ($P < 0.001$), tumor size ($P < 0.05$) and K19 expression ($P < 0.001$) (Table 1). No correlation was found with etiology, differentiation grade or cirrhosis. PDGFRα expression was increased at the invasive front in 54.5% of the cases (48/88; $P < 0.0001$), especially in HCCs displaying microvascular invasion (44/80; $P < 0.0001$) (Figures 1a and b). In all, 26.1% of the PDGFRα-negative HCCs (12/46) were diagnosed as early HCC compared with only 3.3% of the PDGFRα-positive samples (3/90), suggesting that PDGFRα expression may be linked with tumor progression. As the surgical samples were obtained from patients undergoing resection or transplantation, an end-stage treatment, the prognostic value of PDGFRα was analyzed in a cohort of 46 diagnostic needle biopsies with a follow-up exceeding 5 years. In this cohort, PDGFRα expression correlated with poor overall survival ($P < 0.01$) (Figure 1c) and K19 expression ($P < 0.05$) (Supplementary Table S1). We recently described the PDGFRα-dependent translational control of LAMB1 through the translocation of the La/SSB from the nucleus to the cytoplasm and by binding of La/SSB to the LAMB1-IRES in a murine model of HCC progression.[13] To examine whether the PDGFRα/LAMB1 mechanism is relevant in human HCC, 15 patient samples with microvascular invasion

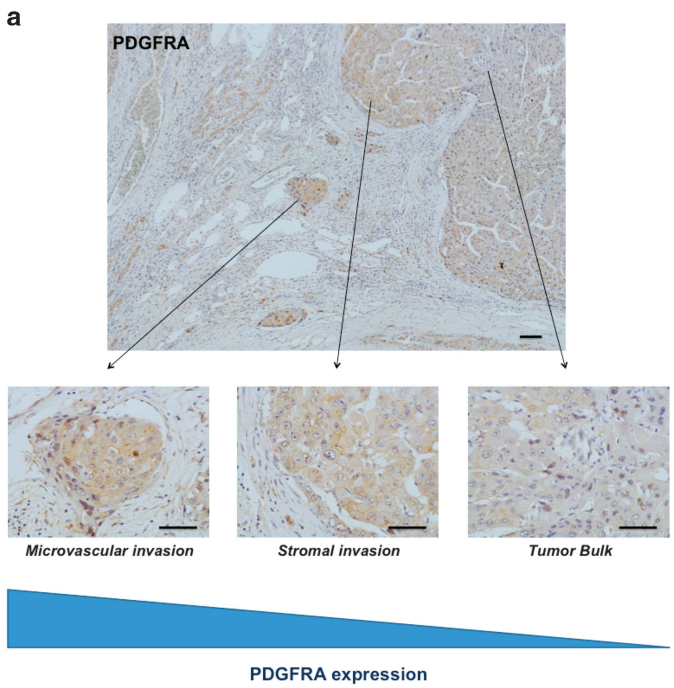

b

Increased PDGFRA expression at invasive front

PDGFRA positivity	No	yes	Totals
no	46	2	48
yes	40	48	88
Totals	86	50	136

Fisher's Exact p<0.0001

Increased PDGFRA expression at invasive front

Microvascular invasion	no	yes	Totals
no	50	6	56
yes	36	44	80
Totals	86	50	136

Fisher's Exact p<0.0001

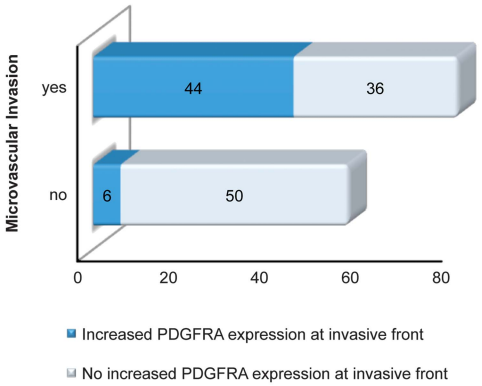

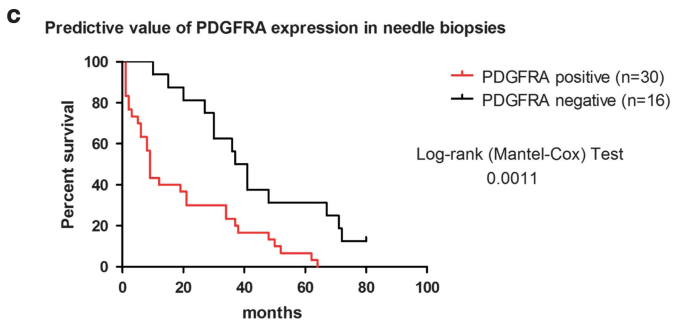

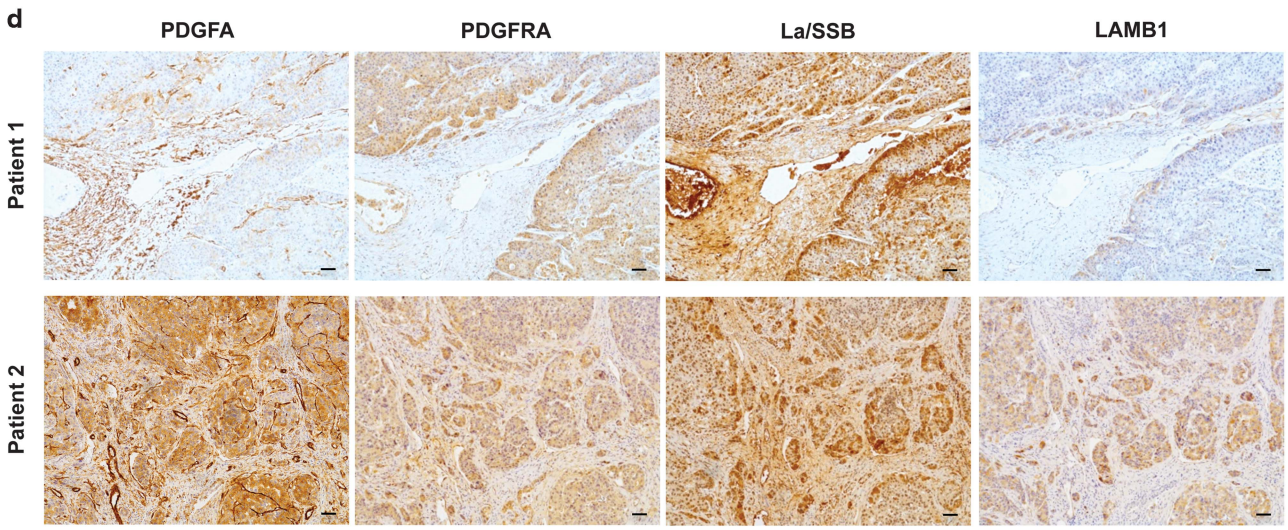

Figure 1. PDGFRα-La/SSB-LAMB1 pathway is expressed at the invasive front of human HCCs. (**a**) Representatitve example of PDGFRα immunohistochemistry in a human HCC sample showing increased expression at invasive front and at sites of microvascular invasion compared with the tumor bulk. (**b**) Diagram, quantification of PDGFRα levels at the tumor bulk, border and at sites of microvascular invasion in surgical HCC samples ($n = 136$). PDGFRα expression is significantly increased at the tumor border and is associated with microvascular invasion (Fisher's exact, $P < 0.0001$). (**c**) Predictive value of PDGFRα expression in needle biopsies ($n = 46$). PDGFRα positivity is associated with a poor overall survival (log-rank Mantel–Cox test, $P = 0.0011$). (**d**) Examples of sequential histological stainings showing the co-expression of PDGFA, PDGFRα, cytosolic La/SSB and LAMB1 in HCCs with microvascular invasion ($n = 15$). Two representative examples (patient 1 and patient 2) with stromal and microvascular invasion show a high expression of members of the PDGFRα-La/SSB-LAMB1 cascade.

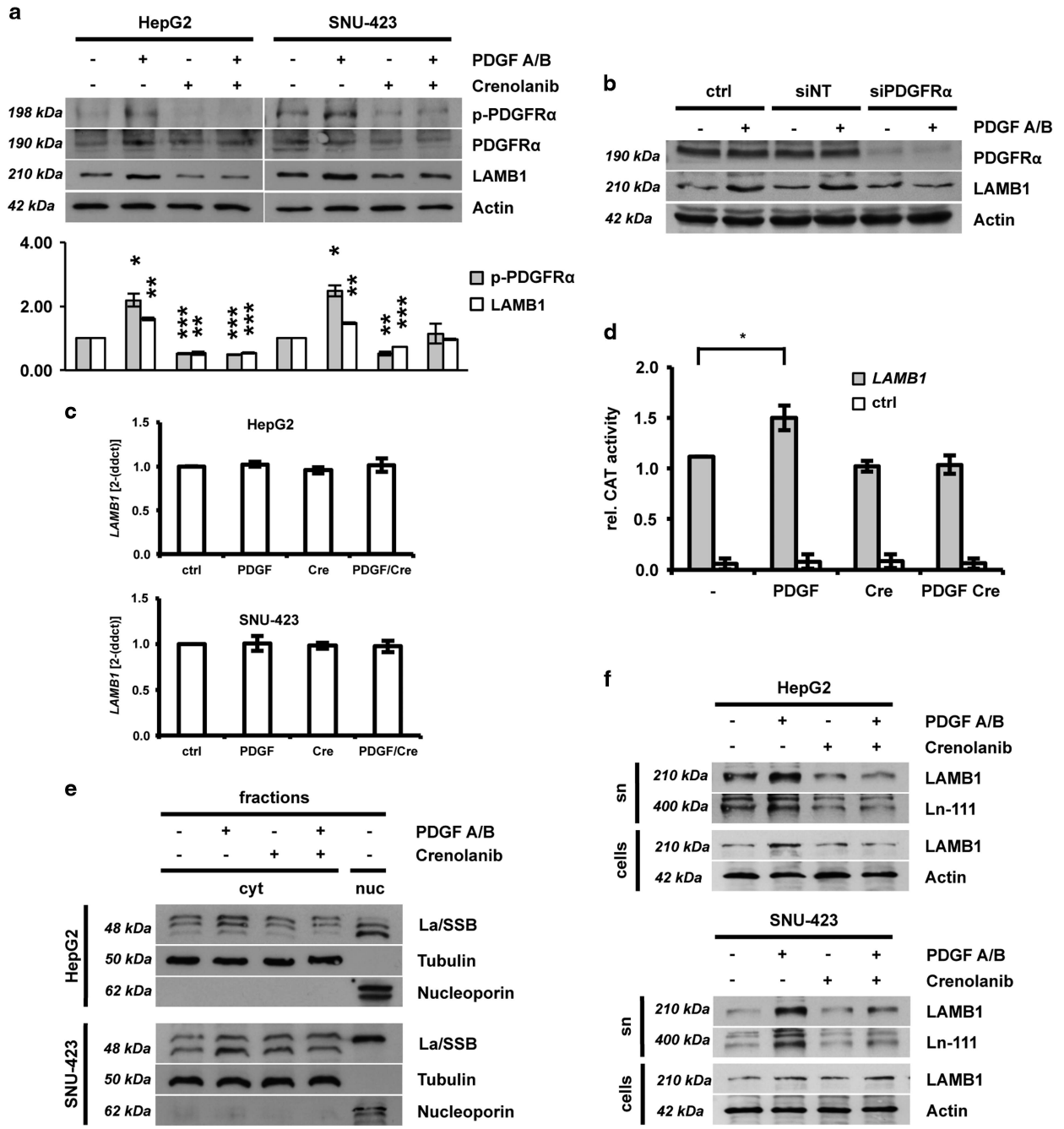

Figure 2. IRES-mediated translation of LAMB1 is enhanced by PDGF**.** HepG2 and SNU-423 cells were treated for 24 h with PDGFA/B ligand or crenolanib, a specific inhibitor of PDGFRα activation. Cells were additionally stimulated with PDGFA/B 15 or 30 min before cell lysis. (**a**) Western blot analysis showing PDGFRα phosphorylation and expression of LAMB1. Actin was used as loading control. The diagram in the lower panel shows relative values of pPDGFRα/PDGFRα and LAMB1/Actin of the quantified western blot ($n = 3$). Signal intensities of untreated cells were set to a value of 1 for normalization. (**b**) Western blot analysis shows that small interfering RNA (siRNA)-mediated knockdown of PDGFRα in HepG2 cells inhibits the increase of LAMB1 expression upon PDGF A/B treatment. A non-targetting siRNA (siNT) was used as a control ($n = 3$). (**c**) qPCR of *LAMB1* expression ($n = 4$). (**d**) HepG2 cells were transfected with a bicistronic vector containing the *LAMB1* 5′-UTR in the intercistronic region between the upstream β-galactosidase (β-gal) and downstream chloramphenicol acetyltransferase (CAT) reporter. Reporter activities were measured 48 h after transfection ($n = 3$). CAT reporter levels showing IRES activity were normalized to β-gal levels representing the transfection efficiency. The empty vector was used for control (ctrl). (**e**) The subcellular localization of La/SSB was analyzed by western blotting of cytoplasmic (c) and nuclear (n) fractions ($n = 3$). Tubulin and nucleoporin served as cytoplasmic or nuclear marker. (**f**) Western blot analysis showing LAMB1 and Ln-111 levels in cell lysate (cells) or supernatant (sn) ($n = 3$). Actin was used as loading control. All data are presented as means ± s.d. and analyzed using the Student's *t*-test (*$P < 0.05$, **$P < 0.01$, ***$P < 0.005$).

were sequentially stained for PDGFα, PDGFRα, La/SSB and LAMB1. PDGFα was strongly expressed in blood vessels surrounding the tumor and was seen focally on the membrane of tumor cells at the invasive front (Figure 1d). In addition, the invasive front not only showed a high PDGFRα expression but also a strong cytoplasmic La/SSB expression compared with the bulk of the tumor where a nuclear La/SSB expression was predominant (Figure 1d, Supplementary Figure S1). In areas with

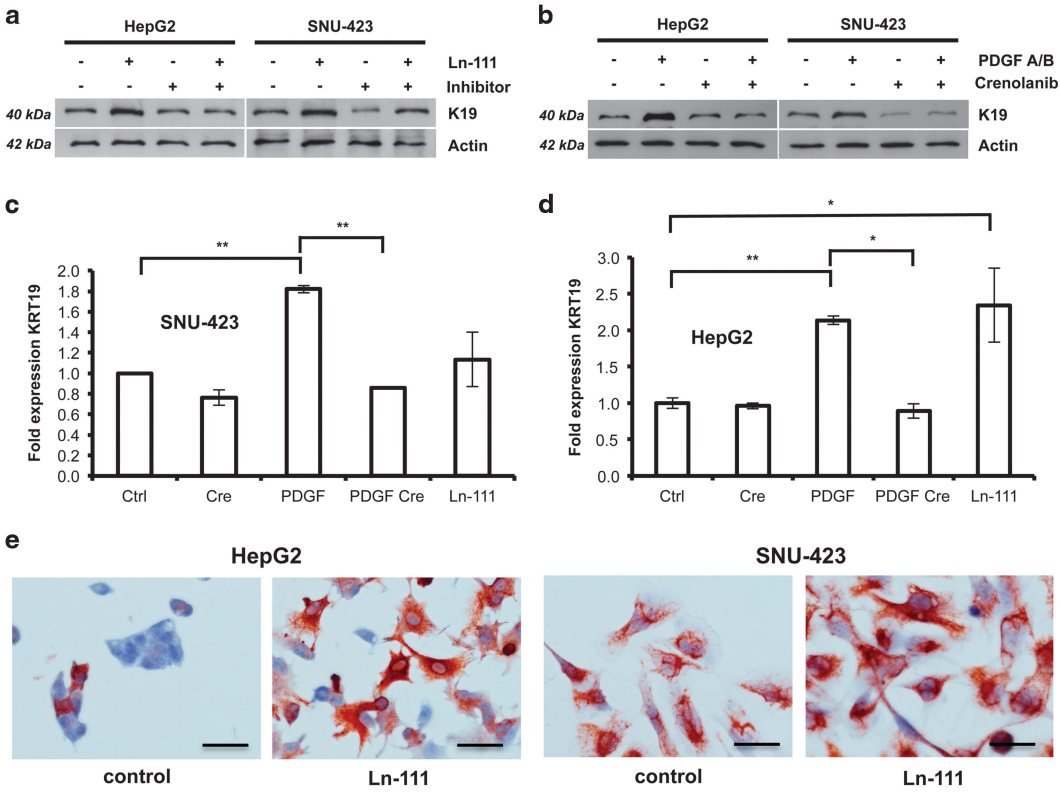

Figure 3. Secretion of Ln-111 stimulates K19 expression. (**a**) HepG2 and SNU-423 cells were cultured on plastic or Ln-111-coated dishes in the presence or absence of an inhibitory antibody specific for Ln-111. Lysates were taken after 24 h and analyzed for K19 expression by western blotting ($n=3$). (**b**) Western blot analysis of cells treated with PDGFA/B or PDGFRα inhibitor crenolanib for 24 h ($n=3$). (**c, d**) qPCR analysis of cells treated with PDGFA/B, crenolanib or Ln-111 coating. ($n=4$, data are presented as means ± s.d. and analyzed using the Student's *t*-test, $^{*}P<0.05$, $^{**}P<0.01$) (**e**) The effect of Ln-111 coating on K19 expressing was visualized using immunocytochemistry ($n=4$, Scale bar 100 μm).

cytoplasmic La/SSB positivity, LAMB1 expression was observed in the cytoplasm and the extracellular surroundings of tumor cells, indicating that the PDGFRα-La/SSB-LAMB1 signaling pathway is active at the invasive front.

PDGF regulates Ln-111 secretion in human HCC cell lines

In order to validate the results observed in human samples, the PDGFRα-La/SSB-LAMB1 cascade was investigated *in vitro*. HepG2 and SNU-423 human hepatoma cells expressed detectable levels of both PDGFRα and PDGFRβ on RNA and protein level (Supplementary Figure S2). Both HCC cell types responded to PDGFA/B stimulation by Y754-phosphorylation of PDGFRα and increased expression of LAMB1 (Figure 2a). This effect was abolished by simultaneous treatment with the specific PDGFRα inhibitor crenolanib, indicating that LAMB1 expression depends on the activation of PDGFRα.[17]

Albeit PDGFRβ is expressed at low levels in HepG2 compared with SNU-423, both cell lines respond to PDGFA/B stimulation with a comparable upregulation of LAMB1 expression. Knockdown of PDGFRα in HepG2 abolished the effect of PDGFA/B, indicating that PDGFRα is the limiting factor in regulating LAMB1 expression (Figure 2b). Quantitative PCR (qPCR) analysis revealed that the mRNA expression of *LAMB1* is not affected by the modulation of the PDGF signaling, suggesting a regulation at the level of mRNA translation (Figure 2c). Thus, we analyzed the IRES regulation of *LAMB1* with a bicistronic reporter assay and found that the *LAMB1*-IRES activity is enhanced by PDGF stimulation (Figure 2d). This effect was reduced in the presence of the crenolanib. Accordingly, the cytoplasmic accumulation of La/SSB was induced by PDGFA/B and impaired by crenolanib treatment in both HepG2 and SNU-423 cells, as shown by the shifts of western blot signals—because of posttranslational modifications—from nuclear to cytoplasmic fractions (Figure 2e). As LAMB1 is the β1-subunit of laminin-111 (Ln-111), which is the predominant laminin isoform found in the liver, we next questioned whether the LAMB1 assembling into Ln-111 is regulated by PDGF. Immunodetection of whole-cell lysates and cell culture supernatants revealed that PDGF elevated LAMB1 expression and resulted in increased secretion of Ln-111 (Figure 2f). Taken together, these data show that activation of PDGFRα signaling triggers the translocation of nuclear La/SSB into the cytoplasm where it enhances LAMB1-IRES translation. Enhanced LAMB1 expression leads to increased secretion of Ln-111.

K19 expression is driven by an autocrine Ln-111 loop

As PDGFRα expression significantly correlated with K19 expression (Table 1 and Supplementary Table S1), we investigated whether PDGFRα-La/SSB-LAMB1/Ln-111 and K19 regulation are molecularly linked. Western blot and immunocytochemical analyses showed that HepG2 and SNU-423 cells respond to Ln-111 treatment by upregulating K19 expression (Figures 3a and e). K19 levels were reduced by the simultaneous treatment with an inhibitory Ln-111 antibody. In addition, PDGFA/B elevated K19 expression was reduced in the presence of crenolanib (Figure 3b). PDGFA/B and Ln-111 stimulation induced *KRT19* mRNA, indicating regulation at transcriptional level (Figures 3c and d). *In silico* analysis identified TEA domain transcription factor 4 (TEAD4) as a candidate transcriptional regulatory element of *KRT19* (Supplementary Table S2 and Supplementary Figure S3). Upon Ln-111 coating, TEAD4 shifted from the cytoplasm to the nucleus, suggesting transcriptional activity (Supplementary Figure S3). Treatment with collagen-1, which can partly signal through the same integrin (ITG)

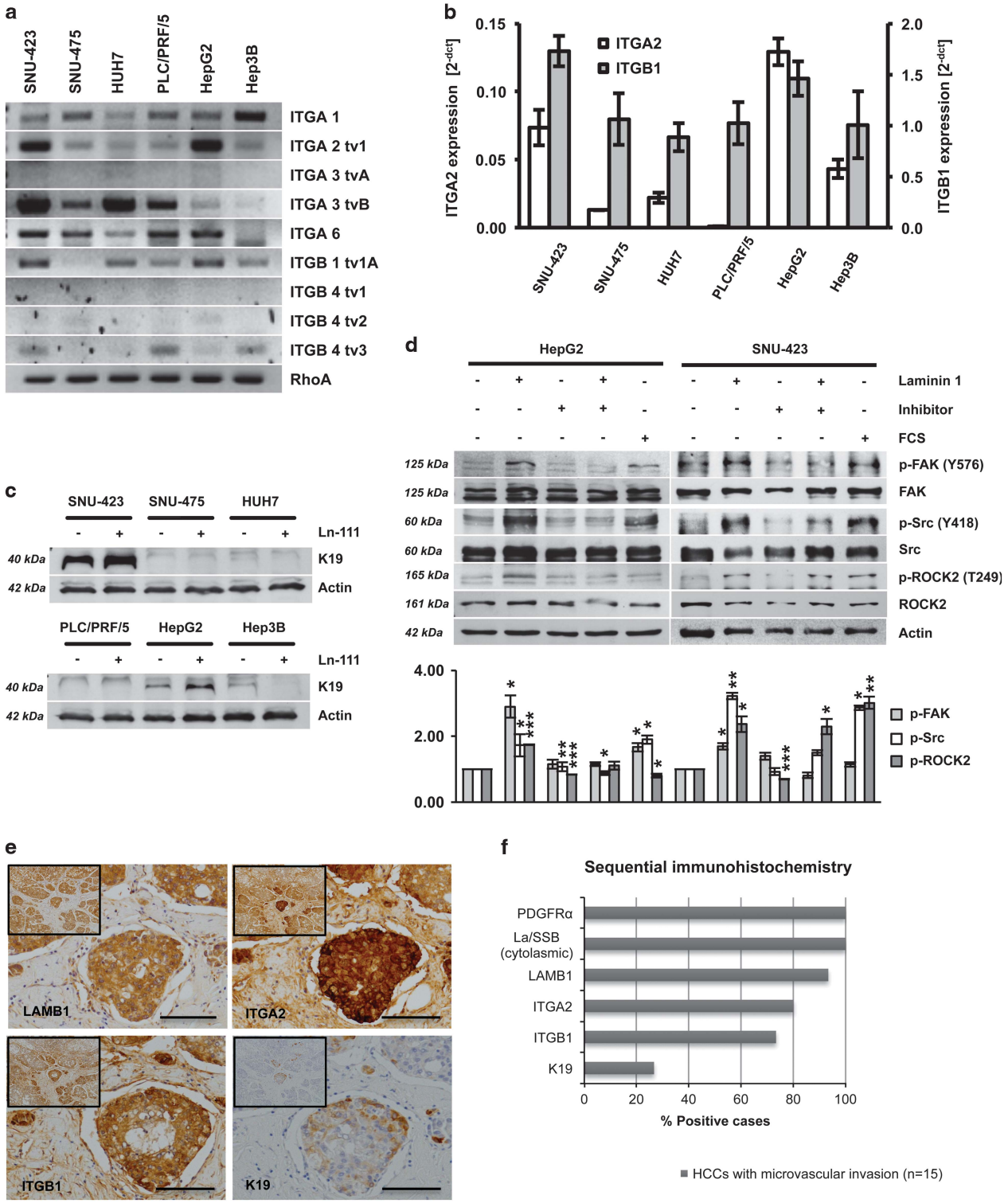

Figure 4. Ln-111 activates ITG signaling and downstream ROCK2. (**a**) HCC cell lines were analyzed for ITG receptor expression by PCR or (**b**) qPCR. (**c**) K19 levels of HCC cell lines cultured on plastic or Ln-111-coated dishes were detected by western blot analysis. (**d**) HepG2 and SNU-423 cells were cultured on plastic or Ln-111-coated dishes in the presence or absence of an inhibitory antibody specific for Ln-111. The medium was replaced with serum-free medium after 12 h. Lysates were taken after 24 h and analyzed by western blotting. For the fetal calf serum (FCS)-positive control, 10% FCS were added to the media 30 min before cell lysis. Ln-111 coating induced the phosphorylation of ITG-specific downstream proteins focal adhesion kinase (FAK), Src and ROCK2. The diagram in the lower panel shows relative values of pFAK/FAK, pSrc/Src and pROCK2/ROCK2 of the quantified western blot ($n=3$). Signal intensities of untreated cells were set to a value of 1 for normalization. (**e**) Representative HCC sample showing strong positivity for LAMB1, ITGA2 and ITGB1, and focal positivity for K19 in invading tumor cells located in a blood vessel (scale bars 100 μm). (**f**) Sequential stainings for PDGFRα, cytosolic La/SSB, LAMB1, ITGA2, ITGB1 and K19 were performed on 15 HCC samples with microvascular invasion and scored for immunopositivity. All data are presented as means ± s.d. and analyzed using the Student's *t*-test (*$P < 0.05$, **$P < 0.01$, ***$P < 0.005$).

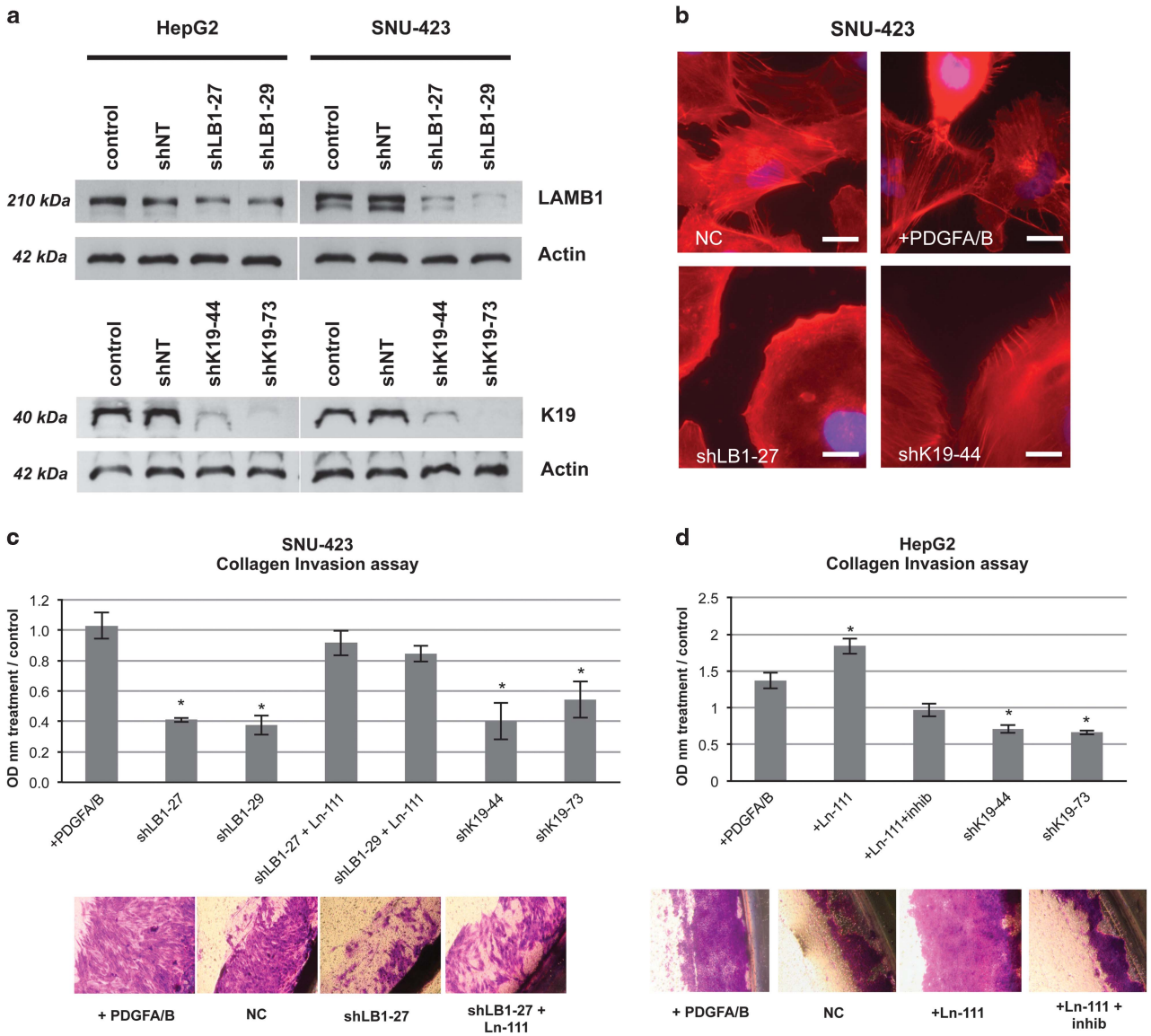

Figure 5. Ln-111 promotes invasion and invadopodia formation. (**a**) Expression of short hairpin RNA (shRNA) targeting *LAMB1* (shLAMB-27, shLB1-29) or *KRT19* (shK19-44, shK19-73) resulted in a stable knockdown and reduced protein expression as shown western blotting. Non-target shRNA (shNT) was used as control. (**b**) LAMB1 (shLB1-27) or K19 (shK19-44) knockdown reduced the formation of invadopodia in SNU-423 cells, whereas PDGF A/B treatment slight increased invadopodia (NC, negative control; scale bars 50 μm). (**c, d**) SNU-423 and HepG2 cells were subjected to a collagen Boyden chamber-based invasion assay ($n=3$, $t=72$ h). OD, optical density; all data are presented as means ± s.e.m. relative to the untreated control and analyzed using the Student's *t*-test compared to the control (*$P<0.05$).

receptors as Ln-111, did not affect K19 expression (Supplementary Figure S4). From these data, we conclude that extracellular Ln-111 activates K19 expression.

K19 is inducible in α2β1 ITG-positive HCC cells

Ln-111 mainly signals by binding to ITG receptors. Several HCC cell lines were analyzed for ITG expression using PCR/qPCR to investigate which receptors correlate with Ln-111-induced K19 expression (Figures 4a and b). HepG2 and SNU-423 cells showed high expression of the subunits *ITGA2* and *ITGB1*, which can form the α2β1 ITG receptor. Notably, only these cell lines responded to Ln-111 stimulation by upregulation of K19 (Figure 4c). Furthermore, Ln-111 activated the ITG-dependent focal adhesion kinase/Src proto-oncogene non-receptor tyrosine kinase (Src) signaling and the ITG-specific downstream target Rho-associated coiled-coil containing protein kinase 2 (ROCK2, Figure 4d). Sequential immunohistochemical stainings in human HCC samples with microvascular invasion ($n=15$) showed a strong positivity for ITGA2 and ITGB1 at the invasive front, where also LAMB1 was noted (Figures 4e and f). K19 showed a focal positivity at the invasive front of four HCCs, suggesting that K19 is a sign of advanced tumor progression (Figure 4e and Supplementary Figure S1). In addition, the prognostic value of *ITGA2*, *ITGB1*, *TEAD4* and *KRT19* gene expression was validated in a cohort of 370 human patients obtained from the Cancer Genome Atlas. The four-gene signature stratified patients into groups with poor overall survival ($n=370$, $P<0.05$) and early recurrence ($n=319$, $P<0.01$) (Supplementary Figure S5).

LAMB1/Ln-111 promotes invasion and invadopodia formation

As LAMB1 is detected at the invasive front of human HCCs and induces K19 expression, a marker associated with microvascular invasion and metastasis, we investigated the functional role of LAMB1 on cell invasion. Stable transfection of the SNU-423 cells and

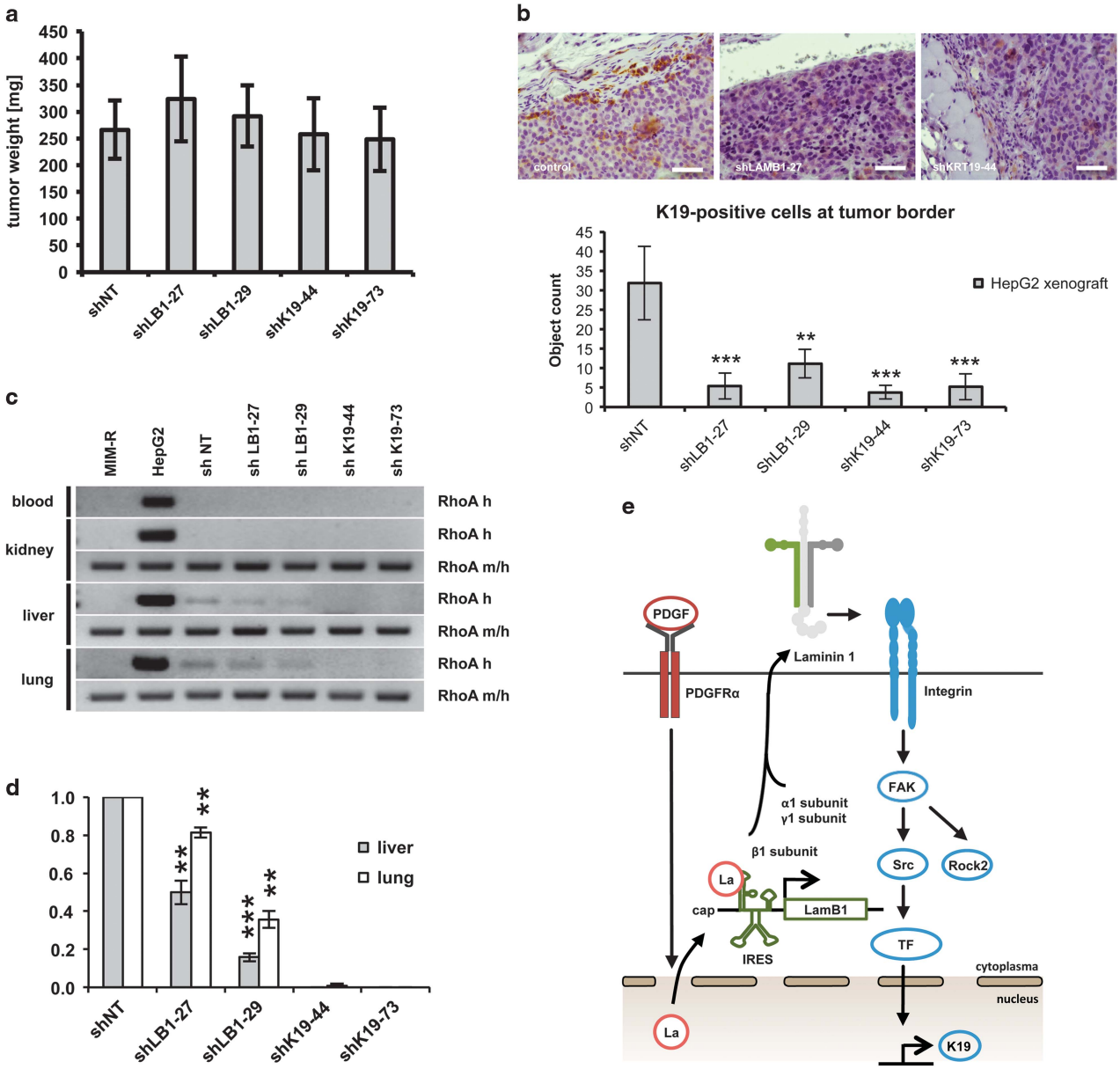

Figure 6. LAMB1 and K19 promote metastatic colonization. (**a**) HepG2 cells with a knockdown of LAMB1 (shLB1-27, shLB1-29) or K19 (shK19-44, shK19-73) or the non-target control (shNT) were subcutaneously injected into NSG mice. Shown are the average weights of resected tumors ($n=8$) after 50 days. (**b**) Immunohistochemical analysis showed a reduced number of single K19-positive cells undergoing stromal invasion upon LAMB1- or K19- knockdown in the subcutaneous HepG2 xenograft mouse model (scale bars 100 μm). Cells at the tumor border were quantified in five different high-power field. (**c**) HepG2 cells were injected into the tail vein of NSG mice ($n=4$). Blood samples and organs were taken after 42 days. Samples were homogenized, pooled and analyzed by PCR. The presence of HepG2 cells was determined with a human-specific primer (RhoA h). Primers recognizing human as well as mouse RhoA (m/h) were used for normalization. Cultured murine (MIM-R) and human (HepG2) cells were used as control. (**d**) RNA levels were quantified by ImageQuant software. Signal intensities of shNT were set to a value of 1 for normalization. (**e**) Schematic overview. PDGFRα activation by PDGF A/B triggers the translocation of La/SSB from the nucleus to the cytoplasm. La/SSB acts as ITAF and binds to the untranslated region of the *LAMB1* mRNA to enhance IRES translation. LAMB1 joins with α- and γ-subunits to form Ln-111. The secreted Ln-111 activates (α2β1) ITG driven focal adhesion kinase (FAK)/Src signaling and regulates ROCK2 phosphorylation and K19 expression. All data are presented as means ± s.d. and analyzed using the Student's *t*-test (*$P<0.05$, **$P<0.01$, ***$P<0.005$).

HepG2 cells with short-hairpins directed against *LAMB1* and *KRT19* resulted in lower protein expression (Figure 5a). Both LAMB1- and K19-knockdown reduced invadopodia formation in SNU-423 cells, whereas PDGFA/B treatment mildly stimulated formation (Figure 5b). As SNU-423 cells express a high basal level of K19 (Figure 3e), we used the SNU-423 cells as a model for Ln-111 inhibition, whereas HepG2 cells were used as a model for Ln-111 stimulation. The LAMB1 knockdown resulted in a reduced capacity to invade through a collagen membrane in the SNU-423 cells (Figure 5c). This effect was restored when coating the collagen Boyden chamber with Ln-111 before seeding (Figure 5c). Ln-111 coating promoted invasion in the HepG2 cells, which was repressed upon anti-Ln-111 antibody treatment (Figure 5d). Knockdown of K19 reduced the capacity to invade in both cells, when compared with the untreated control.

LAMB1 and K19 provide metastatic features *in vivo*

We addressed the question whether K19 is in addition to being a marker for patient survival actively involved in regulating tumor progression. The effect of LAMB1- and K19-knockdown in hepatoma cells was analyzed for tumor formation after xenografting. As SNU-423 cells were not tumorigenic, all *in vivo* experiments were performed with HepG2 cells. Neither the knockdown of LAMB1 nor of K19 influenced subcutaneous tumor growth of HepG2 cells (Figure 6a and Supplementary Figure S6). In accordance, we found that K19 or LAMB1 knockdown had no effect on cell proliferation *in vitro* (Supplementary Figure S7). In the control tissue derived from parental HepG2 cells, a few K19-positive cells underwent stromal invasion at the tumor border, which was lost upon knockdown of K19 or LAMB1 (Figure 6b). We further analyzed the ability of LAMB1- or K19-targeted HepG2 cells for metastatic colonization after tail vein injection. Blood samples and organs were analyzed by PCR with primers specific for human RhoA. Primers that detect both human and mouse RhoA were used for normalization. This analysis showed that knockdown of K19 significantly reduced HepG2 colonization into the lung and liver (Figures 6c and d), suggesting that intervention with K19 expression negatively affects the abilities of HCC cells to extravasate and colonize distal tissues.

DISCUSSION

The expression of PDGFRα has previously been associated with metastasis and increased recurrence in patients diagnosed with HCC.[11,12] *In vitro,* PDGFRα has been reported to promote invadopodia formation and invasion, though the exact mechanism is unclear.[18] Using a large cohort of HCC samples, this study shows that PDGFRα expression was strongly associated with microvascular invasion, metastatic spread and K19 expression. PDGFRα expression was especially increased at the tumor border, implying a communication between the tumor and its surroundings. The ligand PDGFα was strongly expressed by surrounding blood vessels suggesting that endothelial cells may influence tumor behavior. Abnormal angio-architecture and angiogenesis is distinctive for end-stage liver cirrhosis and may be necessary to sustain HCC progression.[19,20] Our results shows that activation of PDGFRα leads to LAMB1 deposition in a La/SSB-dependent manner, irrespective of the levels of PDGFRβ. We suggest that PDGFRα signaling activates the translocation of La/SSB from the nucleus to the cytoplasm where it interacts with the IRES motif of LAMB1 mRNA, enhancing the translation, which results in an increased expression of Ln-111 (Figure 6e). In human HCC samples, a cytoplasmic La/SSB and LAMB1 positivity was mainly seen in invasive epithelial tumor cells, indicating that these cells generate their own microenvironment. Many subtypes of laminins have been described to promote cell adhesion and migration via ITG interaction.[21] Our results show that LAMB1 has an effect on HCC cell lines expressing the α2β1 ITG receptor by activating focal adhesion kinase/Src and ROCK2. ROCK2 is a regulator of the actin cytoskeleton and cell polarity and has been implemented in metastasis and invasion of human HCC.[22] In addition, LAMB1 induces a phenotype switch resulting in increased expression of the biliary/HPC marker K19, probably regulated by the transcription factor TEAD4. TEAD4 can form a binding complex with yes-associated protein 1, which has been reported to induce hepatic progenitor features in regenerating liver and to be a downstream target of ITGB1 in activated hepatic stellate cells.[23,24] Our results show that the *ITGA2-ITB1-TEAD4-KRT19* gene signature has prognostic value, presumably reflecting the activation of the PDGFRα cascade in α2β1 ITG-positive human HCC.

The occurrence of K19, a biliary/HPC marker, has been widely described as a poor prognostic marker in human HCC as it correlates with microvascular invasion, metastatic spread, poor differentiation, early recurrence and consequently poor overall survival.[16,25–28] It has been an on-going debate whether K19 reflects an HPC origin or is a sign of tumor progression. Using a diethylnitrosamine-induced liver tumor mouse model, Mu and colleagues[29] showed that K19 arises because of dedifferentiation rather than finding its origin in an HPC. This study supports the finding that K19 is inducible but, moreover, it shows that LAMB1-mediated K19 expression correlates with invasion and metastasis. Why tumor cells start expressing K19 is still not completely clear. One explanation may be that specific members of the cytoskeleton act as an anchor point for actin filaments to form invadopodia and promote invasion and hence explains the phosphorylation of ROCK2. Another hypothesis may be that tumor cells are protecting themselves by inducing K19 and 'educating' themselves for successful metastasis. In chronic liver disease, hepatocytes can dedifferentiate under stress by expressing biliary markers, a phenomenon called metaplasia.[30,31] In human HCC, knockdown of K19 has been linked with increased sensitivity to chemotherapy, suggesting that K19 also has a protective role.[15] Our results underline the importance of K19 in metastasis as its loss significantly reduced tumor colonization in different organs.

PDGFRα has been reported to be one of the genes to distinguish dysplastic lesions from early HCC.[32] Histologically, stromal invasion is a diagnostic criterion for the differentiation from high-grade dysplastic nodule toward an early HCC.[33] Although in this study most of the early HCCs displayed no PDGFRα expression on protein level, it is very likely that the PDGFRα-LAMB1 pathway becomes activated during tumor progression. This would explain why K19 is only reported in minority of human HCC and strongly links with features of advanced tumor stage. This offers novel therapeutic possibilities to already intervene at an early stage of the disease by inhibiting PDGFRα, using crenolanib, or by targeting specific ITG receptors (for example, ITGA2).

Nevertheless, showing that K19 is inducible and reflects tumor progression, does not exclude that HPCs can be a source for hepatic cancer.[34] Whether HPCs are more prone to form HCCs or rather mixed HCC/cholangiocellular carcinomas still needs be investigated further. Scattered K19-positive cells found in the tumor bulk of human HCCs have been suggested to harbor 'stemness-like' properties.[34] This underlines the complexity and heterogeneity of human HCCs. At this stage, liver cancer research is limited because of the lack of suitable metastatic mouse HCC models and by the fact that most human HCC samples used for research purposes are obtained through an end-stage treatment (that is, resection or transplantation). In mice, the diethylnitrosamine-induced liver cancer model is widely used but it is a model for tumor initiation and growth, lacking invasion and metastasis. Tail vein injection gives you the opportunity to study circulating tumor cells and possible distant metastases, yet it lacks 'the niche' of a chronic diseased liver to sustain new tumor formation. The SNU-423 cell line proved highly invasive *in vitro* but lacked the capacity to grow subcutaneously. This emphasizes the need for future research to take in account the different stages of liver cancer: that is, carcinogenesis, invasion and metastasis, and this on a background of chronic liver disease.

Overall, this study shows that the PDGFRα-LAMB1 pathway has a crucial role in the invasion and metastasis of human HCC through the induction of K19. Not only have several members of this cascade proven to be of prognostic value, but also these results offer the prospect of targeting the cascade at different levels to treat patients at an earlier stage of the disease.

MATERIALS AND METHODS

Patient selection

In all, 182 formalin-fixed paraffin-embedded HCC samples were included in this study. Patients were diagnosed with HCC based on the WHO

classification and treated at the University Hospitals Leuven between 2004 and 2008. The cohort of 136 surgical specimens was obtained after resection or transplantation. Each patient gave informed consent. In case of multiple nodules per patient (for example, satellite nodules in explant livers), the largest HCC nodule was considered as the representative sample. Marker expression was correlated with clinicopathological parameters: tumor size, tumor differentiation, microvascular invasion and metastasis. Microvascular invasion was scored in the tumor and the surrounding area; positivity for metastasis was established using histopathological evaluation and/or based on available clinical data (100 of the 136). A total of 46 needle biopsies were taken for diagnostic purpose or before a surgical procedure. Patients had a follow-up exceeding 5 years to determine the overall survival. This study was approved by the UZLeuven-KU Leuven Biobank and the ethical committee of the University Hospitals Leuven, Belgium.

Immunohistochemistry

Formalin-fixed paraffin-embedded human and mouse samples were stained using the Bond Polymer Refine Detection kit on the Bond Max autostainer (Leica, Microsystems GmbH, Wetzlar, Germany). Primary antibodies were directed against PDGFA (1:100, Santa Cruz Biotechnology, Dallas, TX, USA, 9974), PDGFRα (1:100, Abcam, Cambridge, UK, ab61219), La/SSB (1:50, Santa Cruz Biotechnology, 33593), LAMB1 (1:100, Santa Cruz Biotechnology, 17763), ITGA2 (1:200, Santa Cruz Biotechnology, 74466), ITGB1 (1:100, Abcam, ab24693) and K19 (1:25, Dako, Glostrup, Denmark, RCK108).

Cell culture

All human hepatoma cell lines were obtained from ECACC (Salisbury, UK) and authenticated by short tandem repeat analysis. Human SNU-423 and SNU-475 cells, and murine MIM-R hepatoma cells were cultured in RPMI 1640 plus 10% fetal calf serum.[10] Human HEP3B, HepG2, HUH7 and PLC/PRF/5 cells were propagated in Dulbecco's modified Eagle's medium plus 10% fetal calf serum at 37 °C and 5% CO_2. Cell lines were tested monthly for mycoplasma contamination using MycoFluor Mycoplasma Detection Kit (Invitrogen, Carlsbad, CA, USA). Cells were treated with 20 ng/ml PDGFA/B (PeproTech, Rocky Hill, NJ, USA, 100-00AB) or 50 nM crenolanib (Selleckchem, Houston, TX, USA, CP-868596) for stimulation or inhibition of PDGF signaling, respectively. For stimulation of laminin signaling, culture dishes were coated for 1 h with 10 μg/ml Ln-111 (Sigma-Aldrich, St Louis, MO, USA, L2020) before seeding of the cells, whereas coated dishes were incubated for 30 min with 2 μg/ml anti-laminin 1 antibody (Abcam, ab7463) for inhibition.

Collagen invasion and invadopodia assay

HepG2 or SNU-423 cells were submitted to a QCM Collagen Cell Invasion Assay 8 μm and a QCM Gelatin Invadopodia Assay Green (Millipore, Billerica, MA, USA) according to supplier's protocol. Fetal calf serum was used as attractant; Boyden chambers were coated with 10 μg/ml Ln-111 before seeding. In all, 2 μg/ml anti-laminin 1 antibody (Abcam, ab7463) was used for inhibition of Ln-111, 20 ng/ml PDGFA/B (PeproTech, 100-00AB) for stimulating PDGF signaling.

Immunocytochemistry

Cells were processed into formalin-fixed paraffin-embedded tissue blocks using the Cellient Automated Cell Block System (Hologic, Bedford, MA, USA) and processed for immunohistochemistry as described above. In addition, coated and non-coated cells were stained for K19 (1:50, Dako, RCK108) using Envision Flex anti-mouse secondary (Dako). Visualization was done using 3-amino-9-ethylcarbazole, followed by a hematoxylin counterstaining.

Immunofluorescence

In vitro coated and non-coated cells were stained for TEAD4 (1:50, Abcam, ab58310) and yes-associated protein 1 (1:50, Santa Cruz Biotechnology, 101199), followed by an incubation with a AlexaFluor-488 Goat anti-mouse antibody (Invitrogen). Nuclei were stained with 4′, 6-diamidino-2-phenylindole (Invitrogen).

Transient knockdown of PDGRα

ON-TARGET plus SMARTpool siRNA (Dharmacon, Lafayette, CO, USA) was used to knockdown PDGFRα in HepG2 cells. The cells were transfected with 40 nM small interfering RNA against PDGFRα (L-003162-00-0005) or non-target small interfering RNA (D-001810-10) using Oligofectamin (Invitrogen, 12252011). The transfected cells were treated with 20 ng/ml PDGFA/B (PeproTech, 100-00AB) and cell lysates were further processed for western blot analysis 48 h post transfection.

Stable knockdown of LAMB1 and K19

HepG2 and SNU-423 cells were transduced with MISSION short hairpin RNA lentiviral particles (Sigma-Aldrich) targeting *LAMB1* (TRCN0000315627, TRCN0000083429), *KRT19* (TRCN0000062344, TRCN0000438673). A non-targeting short hairpin RNA vector was used as control. Selection was done by puromycin treatment.

Western blot analysis

Cell lysates were prepared with RIPA buffer (150 mM NaCl, 50 mM Tris pH 7.4, 0.5% sodium-deoxycholate, 1 mM β-glycerophosphate pH 7.2, 1% nonidet P-40) supplemented with proteinase inhibitors (1 mM sodium fluoride, 1 mM sodium orthovanadate, 1 mM phenylmethylsulfonylfluorid, 10 μg/ml leupeptin and 10 μg/ml aprotinin). Nuclear and cytoplasmic fractions were isolated using the previously described REAP method.[35] Protein concentrations were determined by Bradford assay and a total of 20–30 μg protein was used for sodium dodecyl sulfate–polyacrylamide gel electrophoresis. Primary antibodies against LAMB1 (Thermo Fisher Scientific, Waltham, MA, USA, RT-796-P1), PDGFRα (Cell Signaling Technologies, Danvers, MA, USA, 5241), phospho-PDGFRα (Cell Signaling, Technology, 2992), K19 (Thermo Fisher Scientific, MS-1902-P1), Ln-111 (Abcam, ab7463), La/SSB (Santa Cruz Biotechnology, 33593), nucleoporin (BD Biosciences, San Jose, CA, USA, 610498), tubulin (Sigma-Aldrich, T5168), focal adhesion kinase (Santa Cruz Biotechnology, sc-558), phospho-focal adhesion kinase (Invitrogen, 44652G), Src (Cell Signaling, USA, 2109), phospho-Src (Invitrogen, 44660G), ROCK2 (Sigma-Aldrich, HPA007459), phospho-ROCK2 (Abcam, ab83514) and actin (Sigma-Aldrich, A2066) were used at a dilution of 1:1000. Peroxidase-conjugated secondary antibodies (Vector Laboratories, Burlingame, CA, USA, PI-2000, PI-1000 and Santa Cruz Biotechnology, sc-2006) were used for detection at a dilution of 1:10 000. Western blots were quantified using ImageQuant software (Molecular Dynamics, Chatsworth, CA, USA).

Computational analyses

Regulatory elements for *KRT19* were obtained using GeneHancer (http://www.genecards.org/Guide/GeneCard). Multi-gene biomarkers were correlated with clinical outcome in a cohort of 370 patients based upon data generated by the TCGA Research Network: http://cancergenome.nih.gov/. Analysis was performed using the web-based tool cBioPortal.[36,37] Publically available ChIP-seq data for TEAD4 in HepG2 cells (GEO accession GSM1010875) were downloaded from ChIP-Atlas (http://chip-atlas.org/). BigWig and Peak-calls ($q < 1E\text{-}05$) were visualized in the Integrative Genomics Viewer.[38]

Transient transfection and bicistronic reporter assay

The bicistronic construct containing the LAMB1 5'-untranslated region between a β-Gal and chloramphenicol acetyltransferase reporter or the empty control vector were generated as outlined recently.[14] Cells were grown on a six-well plate and transfected with the vectors using Lipofectamine Plus as recommended by the manufacturer (Invitrogen, 18324-020). The cells were lysed 48 h after transfection. β-Galactosidase reporter activity was photometrically determined with o-nitrophenyl-b-D-galactopyranoside. Chloramphenicol acetyltransferase activity was measured by enzyme-linked immunosorbent assay (Roche, Basel, Switzerland, 11363727001) as recommended by the manufacturer. The relative IRES activity was calculated as ratio of chloramphenicol acetyltransferase normalized to β-galactosidase activity.

Subcutaneous tumor formation and tail vein injection

In all, 5×10^6 HepG2 cells were resuspended in 200 μl Ringer solution and subcutaneously injected into 8-week old immunodeficient NSG (NOD.Cg-Prkdc^{scid} Il2rg^{tm1Wjl}/SzJ) female mice ($n = 8$ per group) that were housed in individually vented cages. Tumors were resected after 50 days. In total,

1×10^6 HepG2 cells resuspended in 100 µl Ringer solution were used for tail vein injection ($n = 4$ per group). Blood samples and organs were taken 42 days after injection. Part of the tumor was fixed in formalin and processed into paraffin blocks, the rest of the samples were homogenized, pooled and analyzed by PCR specific for human RhoA. Primers that detect both human and mouse RhoA were used for normalization. Formalin-fixed paraffin-embedded samples were stained as described above. Cells were quantified at the tumor border in five different fields (×200 magnification) using the Nikon Eclipse software (Nikon Instruments Europe BV, Amsterdam, Netherlands). Experiments were performed according to the Austrian guidelines for animal care and protection.

Polymerase chain reaction (PCR) and qPCR

Total RNA was reverse transcribed in complementary DNA as recommended by the manufacturer (Qiagen, Hilden, Germany). Aliquots of complementary DNA were used for PCR using PuReTaq Ready-To-Go PCR beads (GE Healthcare, Little Chalfont, UK, 27-9559-01) and evaluated by agarose gel electrophoresis. PCR signals were densitometrically quantified with ImageQuant 5.0 (GE Healthcare). qPCR was performed with Fast SYBR green (Applied Biosystems, Foster City, CA, USA) and quantified with the 7500 Fast Real-Time PCR System (Applied Biosystems). Primer sequences are shown in Supplementary Table S3.

Statistical analysis

Data were shown as average value ± s.d. The statistical significance of differences was evaluated using an unpaired Student's *t*-test. Significant differences between experimental groups were $^*P < 0.05$, $^{**}P < 0.01$, $^{***}P < 0.005$. Contingency analysis was done using the Fisher's exact test and the unpaired Student's *t*-test with STATVIEW 5.0.1 software (SAS Institute Inc., Cary, NC, USA).

ABBREVIATIONS

IRES, internal ribosome entry site; ITG, integrin; HCC, hepatocellular carcinoma; HPC, hepatic progenitor cell; K/KRT, keratin; LAMB1, laminin beta 1; La/SSB, Sjogren syndrome antigen B; Ln, laminin; PDGF, platelet-derived growth factor; PDGFRα, platelet-derived growth factor receptor α; ROCK2, Rho-associated coiled-coil containing protein kinase 2; Src, Src proto-oncogene non-receptor tyrosine kinase; TEAD4, TEA domain transcription factor 4.

CONFLICT OF INTEREST

The authors declare no conflict of interest.

ACKNOWLEDGEMENTS

This work was supported by the Belgian Federal Science Policy Office, Interuniversity Attraction Poles program—P7/83-HEPRO (to OG), Austrian Science Fund, FWF, T597-B13 (to MP) and P25356 (to WM) and the Belgian Kom op tegen Kanker (to JW). We thank Kathleen Van den Eynde and the Fibrosis Lab, Newcastle University, UK for their indispensible technical support.

REFERENCES

1 Jemal A, Bray F, Center MM, Ferlay J, Ward E, Forman D. Global cancer statistics. *CA Cancer J Clin* 2011; **61**: 69–90.
2 Bruix J, Gores GJ, Mazzaferro V. Hepatocellular carcinoma: clinical frontiers and perspectives. *Gut* 2014; **63**: 844–855.
3 European Association For The Study Of The L, European Organisation For R, Treatment Of C, EASL-EORTC clinical practice guidelines: management of hepatocellular carcinoma. *J Hepatol* 2012; **56**: 908–943.
4 Dhanasekaran R, Venkatesh SK, Torbenson MS, Roberts LR. Clinical implications of basic research in hepatocellular carcinoma. *J Hepatol* 2016; **64**: 736–745.
5 Giannelli G, Rani B, Dituri F, Cao Y, Palasciano G. Moving towards personalised therapy in patients with hepatocellular carcinoma: the role of the microenvironment. *Gut* 2014; **63**: 1668–1676.
6 Villanueva A, Minguez B, Forner A, Reig M, Llovet JM. Hepatocellular carcinoma: novel molecular approaches for diagnosis, prognosis, and therapy. *Annu Rev Med* 2010; **61**: 317–328.
7 Lee JS, Heo J, Libbrecht L, Chu IS, Kaposi-Novak P, Calvisi DF *et al.* A novel prognostic subtype of human hepatocellular carcinoma derived from hepatic progenitor cells. *Nat Med* 2006; **12**: 410–416.
8 Hoshida Y, Nijman SM, Kobayashi M, Chan JA, Brunet JP, Chiang DY *et al.* Integrative transcriptome analysis reveals common molecular subclasses of human hepatocellular carcinoma. *Cancer Res* 2009; **69**: 7385–7392.
9 Hoshida Y, Villanueva A, Kobayashi M, Peix J, Chiang DY, Camargo A *et al.* Gene expression in fixed tissues and outcome in hepatocellular carcinoma. *N Engl J Med* 2008; **359**: 1995–2004.
10 van Zijl F, Mair M, Csiszar A, Schneller D, Zulehner G, Huber H *et al.* Hepatic tumor-stroma crosstalk guides epithelial to mesenchymal transition at the tumor edge. *Oncogene* 2009; **28**: 4022–4033.
11 Wei T, Zhang LN, Lv Y, Ma XY, Zhi L, Liu C *et al.* Overexpression of platelet-derived growth factor receptor alpha promotes tumor progression and indicates poor prognosis in hepatocellular carcinoma. *Oncotarget* 2014; **5**: 10307–10317.
12 Kikuchi A, Monga SP. PDGFRalpha in liver pathophysiology: emerging roles in development, regeneration, fibrosis, and cancer. *Gene Expr* 2015; **16**: 109–127.
13 Petz M, Them NC, Huber H, Mikulits W. PDGF enhances IRES-mediated translation of laminin B1 by cytoplasmic accumulation of La during epithelial to mesenchymal transition. *Nucleic Acids Res* 2012; **40**: 9738–9749.
14 Petz M, Them N, Huber H, Beug H, Mikulits W. La enhances IRES-mediated translation of laminin B1 during malignant epithelial to mesenchymal transition. *Nucleic Acids Res* 2012; **40**: 290–302.
15 Govaere O, Komuta M, Berkers J, Spee B, Janssen C, de Luca F *et al.* Keratin 19: a key role player in the invasion of human hepatocellular carcinomas. *Gut* 2014; **63**: 674–685.
16 Kim H, Choi GH, Na DC, Ahn EY, Kim GI, Lee JE *et al.* Human hepatocellular carcinomas with "stemness"-related marker expression: keratin 19 expression and a poor prognosis. *Hepatology* 2011; **54**: 1707–1717.
17 Heinrich MC, Griffith D, McKinley A, Patterson J, Presnell A, Ramachandran A *et al.* Crenolanib inhibits the drug-resistant PDGFRA D842V mutation associated with imatinib-resistant gastrointestinal stromal tumors. *Clin Cancer Res* 2012; **18**: 4375–4384.
18 Eckert MA, Lwin TM, Chang AT, Kim J, Danis E, Ohno-Machado L *et al.* Twist1-induced invadopodia formation promotes tumor metastasis. *Cancer Cell* 2011; **19**: 372–386.
19 Coulon S, Heindryckx F, Geerts A, Van Steenkiste C, Colle I, Van Vlierberghe H. Angiogenesis in chronic liver disease and its complications. *Liver Int* 2011; **31**: 146–162.
20 Fernandez M, Semela D, Bruix J, Colle I, Pinzani M, Bosch J. Angiogenesis in liver disease. *J Hepatol* 2009; **50**: 604–620.
21 Patarroyo M, Tryggvason K, Virtanen I. Laminin isoforms in tumor invasion, angiogenesis and metastasis. *Semin Cancer Biol* 2002; **12**: 197–207.
22 Wong CC, Wong CM, Tung EK, Man K, Ng IO. Rho-kinase 2 is frequently overexpressed in hepatocellular carcinoma and involved in tumor invasion. *Hepatology* 2009; **49**: 1583–1594.
23 Yimlamai D, Christodoulou C, Galli GG, Yanger K, Pepe-Mooney B, Gurung B *et al.* Hippo pathway activity influences liver cell fate. *Cell* 2014; **157**: 1324–1338.
24 Martin K, Pritchett J, Llewellyn J, Mullan AF, Athwal VS, Dobie R *et al.* PAK proteins and YAP-1 signalling downstream of integrin beta-1 in myofibroblasts promote liver fibrosis. *Nat Commun* 2016; **7**: 12502.
25 Zhuang PY, Zhang JB, Zhu XD, Zhang W, Wu WZ, Tan YS *et al.* Two pathologic types of hepatocellular carcinoma with lymph node metastasis with distinct prognosis on the basis of CK19 expression in tumor. *Cancer* 2008; **112**: 2740–2748.
26 Uenishi T, Kubo S, Yamamoto T, Shuto T, Ogawa M, Tanaka H *et al.* Cytokeratin 19 expression in hepatocellular carcinoma predicts early postoperative recurrence. *Cancer Sci* 2003; **94**: 851–857.
27 Tsuchiya K, Komuta M, Yasui Y, Tamaki N, Hosokawa T, Ueda K *et al.* Expression of keratin 19 is related to high recurrence of hepatocellular carcinoma after radiofrequency ablation. *Oncology* 2011; **80**: 278–288.
28 Yang XR, Xu Y, Shi GM, Fan J, Zhou J, Ji Y *et al.* Cytokeratin 10 and cytokeratin 19: predictive markers for poor prognosis in hepatocellular carcinoma patients after curative resection. *Clin Cancer Res* 2008; **14**: 3850–3859.
29 Mu X, Espanol-Suner R, Mederacke I, Affo S, Manco R, Sempoux C *et al.* Hepatocellular carcinoma originates from hepatocytes and not from the progenitor/biliary compartment. *J Clin Invest* 2015; **125**: 3891–3903.
30 Guldiken N, Ensari GK, Lahiri P, Couchy G, Preisinger C, Liedtke C *et al.* Keratin 23 is a general stress-inducible marker of mouse and human ductular reaction in liver disease. *J Hepatol* 2016; **65**: 552–559.
31 Desmet VJ. Ductal plates in hepatic ductular reactions. Hypothesis and implications. I. Types of ductular reaction reconsidered. *Virchows Arch* 2011; **458**: 251–259.
32 Llovet JM, Chen Y, Wurmbach E, Roayaie S, Fiel MI, Schwartz M *et al.* A molecular signature to discriminate dysplastic nodules from early hepatocellular carcinoma in HCV cirrhosis. *Gastroenterology* 2006; **131**: 1758–1767.
33 International Consensus Group for Hepatocellular NeoplasiaThe International Consensus Group for Hepatocellular N, Pathologic diagnosis of early

hepatocellular carcinoma: a report of the international consensus group for hepatocellular neoplasia. *Hepatology* 2009; **49**: 658–664.

34 Govaere O, Wouters J, Petz M, Vandewynckel YP, Van den Eynde K, Van den Broeck A *et al*. Laminin-332 sustains chemoresistance and quiescence as part of the human hepatic cancer stem cell niche. *J Hepatol* 2016; **64**: 609–617.

35 Suzuki K, Bose P, Leong-Quong RY, Fujita DJ, Riabowol K. REAP: a two minute cell fractionation method. *BMC Res Notes* 2010; **3**: 294.

36 Cerami E, Gao J, Dogrusoz U, Gross BE, Sumer SO, Aksoy BA *et al*. The cBio cancer genomics portal: an open platform for exploring multidimensional cancer genomics data. *Cancer Discov* 2012; **2**: 401–404.

37 Gao J, Aksoy BA, Dogrusoz U, Dresdner G, Gross B, Sumer SO *et al*. Integrative analysis of complex cancer genomics and clinical profiles using the cBioPortal. *Sci Signal* 2013; **6**: pl1.

38 Consortium EP, An integrated encyclopedia of DNA elements in the human genome. *Nature* 2012; **489**: 57–74.

Supplementary Information accompanies this paper on the Oncogene website (http://www.nature.com/onc)